EUROPHYSICS LETTERS 15 April 2000

Europhys. Lett., **50** (2), pp. 189–195 (2000)

Phonon-like and single-particle dynamics in liquid lithium

T. Scopigno[1], U. Balucani[2], A. Cunsolo[3], C. Masciovecchio[3], G. Ruocco[4], F. Sette[3] and R. Verbeni[3]

[1] *Università di Trento and Istituto Nazionale di Fisica della Materia I-38100, Trento, Italy*
[2] *Istituto di Elettronica Quantistica, Consiglio Nazionale delle Ricerche I-50127, Firenze, Italy*
[3] *European Synchrotron Radiation Facility - B.P. 220 F-38043 Grenoble, Cedex France*
[4] *Università di L'Aquila and Istituto Nazionale di Fisica della Materia I-67100, L'Aquila, Italy*

(received 22 October 1999; accepted in final form 31 January 2000)

PACS. 61.25.Mv – Liquid metals and alloys.
PACS. 61.10.Eq – X-ray scattering (including small-angle scattering).
PACS. 61.20.Ne – Structure of simple liquids.

Abstract. – The dynamic structure factor, $S(Q,E)$, of liquid lithium ($T = 475\,\mathrm{K}$) has been remeasured by inelastic X-ray scattering (IXS) in an extended momentum transfer region ($Q = 1.4$–$110\,\mathrm{nm}^{-1}$) and with improved energy resolution (down to 1.5 meV). These new data on such prototypical simple liquid allow to observe the full evolution with Q from a phonon-like collective mode towards the single-particle dynamics. As a function of Q, one finds: i) at low Q's, a sound mode with a positive dispersion of the sound velocity, ii) at intermediate Q's, excitations whose energy oscillates similarly to phonons in the crystal Brillouin zones, and iii) at high Q's, the $S(Q,E)$ approaches a Gaussian shape, indicating that the single-particle dynamics has been reached.

The spectrum of density fluctuations, $S(Q,E)$, of a liquid shows a very rich phenomenology with features strongly dependent on the considered momentum, Q, and energy, E, regions. The shape of the $S(Q,E)$ is well established in the low- and high-Q limits [1–4]. In the hydrodynamic limit, *i.e.* at $Q/Q_{\mathrm{M}} \ll 1$ (Q_{M} is the position of the first maximum of the static structure factor $S(Q)$), the spectrum shows three peaks —the Brillouin triplet. They are, respectively, the Stokes and anti-Stokes propagating compressional modes —dispersing linearly with the adiabatic sound velocity v_{s}— and the thermal diffusion mode centered at zero energy transfer. In the opposite limit, *i.e.* at $Q/Q_{\mathrm{M}} \gg 1$, one reaches the so-called impulse approximation, where the excited particle acquires a kinetic energy much higher than any inter-particle potential energy. Therefore the target particle behaves as a free particle, and the $S(Q,E)$ lineshape reflects the particles' initial state momentum distribution. Considering the Boltzmann distribution, the $S(Q,E)$ reduces to a Gaussian centered at the recoil energy $\hbar^2Q^2/2M$, and with variance $\hbar^2K_{\mathrm{B}}TQ^2/M$. Here, M is the particle mass. The evolution between these two limit cases is affected by a realm of dynamical processes [3]. One has, for example, the interaction of sound waves with other degrees of freedom (translational diffusion, rotations and internal modes for molecules), and the interaction among different collective modes, responsible, for example, for the slowing-down of the diffusional dynamics in supercooled liquids. Moreover, when Q is comparable to Q_{M}, one should consider that important modifications of the Brillouin triplet occur also as a consequence of structural

effects. In fact, the sound waves in the liquid can no longer be described as density fluctuation of a continuum medium, and the local structure with its intrinsic disorder becomes relevant. Finally, compared to the crystalline case, the absence of long-range order will prevent to a certain extent, in the liquid, the replication of the sound dispersion relation in high-order Brillouin Zones (BZ).

This rich phenomenology has long motivated the study of the dynamics of liquid systems using both experimental, numerical and theoretical techniques. Using ultrasound absorption methods and Brillouin light scattering techniques, the sound waves, and their interactions with the relaxation processes active in the liquid, have been studied in great detail up to $Q/Q_{\mathrm{M}} \approx 10^{-3}$. Similarly, Inelastic Neutron Scattering (INS) has been used at very large Q transfers to determine the $S(Q,E)$ in the impulse approximation [4]. INS and numerical methods have also been extensively used to study the $S(Q,E)$ in the Q region close to Q_{M}, where the two limit descriptions are expected to fail [5,6]. In this region one finds important differences in the shape of the $S(Q,E)$ of different dense simple fluids as, for example, noble gases and liquid metals. Among them, for example, in noble gas the $S(Q,E)$ is an almost featureless peak at Q comparable to Q_{M} [7], while for the metals it is still possible to identify an inelastic feature even above Q_{M} [8]. The kinematic limitations on the accessible Q-E region of existing INS instruments [9] did not allow to study with continuity and under comparable experimental conditions the liquid dynamics in the Q-range spanning from the collective to the single-particle behaviors. Moreover, the neutron scattering cross-section accounts for two different contributions: besides the coherent cross-section —probing the collective dynamics— there is an incoherent contribution which, at each wave vector, reflects the single-particle motion and therefore hides the crossover between the previously quoted regimes. The devolepment of Inelastic X-ray Scattering (IXS) [10,11] has allowed, recently, to sensibly extend the accessible Q-E region in disordered materials and to avoid the incoherent contribution.

In this work we report the determination by IXS of the dynamic structure factor of liquid lithium in the 1.4–110 nm^{-1} Q-range, corresponding to $Q/Q_{\mathrm{M}} \approx 5 \cdot 10^{-2}$–5. Lithium has been chosen because, among the simple monoatomic liquids, is the one that is best suited to IXS [10,12]. Indeed, its low mass gives recoil energies observable in the considered Q-range, and its low atomic number and large sound velocity ($\approx 5000\,\mathrm{m/s}$) give optimal signal with the available energy resolution, compensating for the large form factor decrease at high Q values [13]. The $S(Q,E)$ spectra, reported to their absolute scale exploiting the zeroth and first moments sum rules, show the transition from a triplet to a Gaussian. The maxima, $\Omega(Q)$, of the longitudinal current spectra ($E^2/Q^2 S(Q,E)$) show an almost linear dispersion relation at low Q —typical of a sound wave— and a completely different dependence in the high-Q limit, where it approaches the parabolic dispersion of the free particle. These two regions are joined by oscillations of $\Omega(Q)$, which are in phase with the structural correlations, as observed in the $S(Q)$. Finally, in the low-Q region these data confirm the existence of positive dispersion of the sound velocity. Contrary to the previous findings [12], however, the higher accuracy of the present data allows to establish that the transition between the normal and fast sound regimes does not take place at $Q = 3.6\,\mathrm{nm}^{-1}$, but at sensibly lower Q values.

The experiment has been carried out at the very high energy resolution IXS beamline ID16, at the European Synchrotron Radiation Facility. The incident X-ray beam is obtained by a back-scattering monochromator operating at the Si($h\ h\ h$) ($h = 7, 9, 11$) reflections [14]. The scattered photons are collected by spherical silicon crystal analyzers, operating at the same Si($h\ h\ h$) reflection [15]. The total energy resolution —obtained from the measurement of $S(Q_{\mathrm{M}},E)$ in a Plexiglas sample which is dominated by elastic scattering— is 8.5 meV full-width half-maximum for $h = 7, 3\,\mathrm{meV}$ for $h = 9$ and 1.5 meV for $h = 11$. The momentum transfer, $Q = 2k_h \sin(\theta_{\mathrm{s}}/2)$, with k_h the wave vector of the incident photon and θ_{s} the scat-

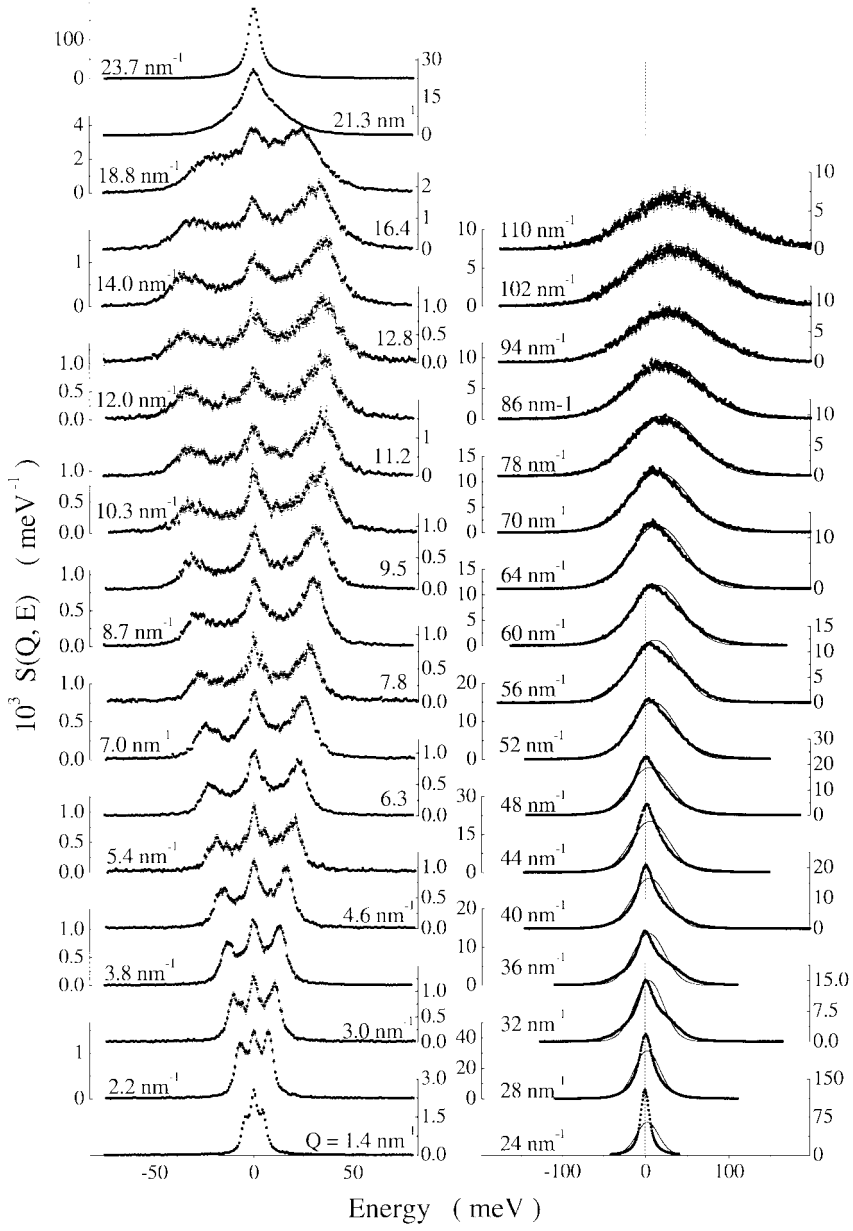

Fig. 1 – Dynamic Structure Factor (Density Correlation Function) of lithium at $T = 475\,\mathrm{K}$ measured by IXS and normalized according to the procedure discussed in the text. The spectra on the left column are taken with a resolution $\Delta E = 3$ meV using Si (9 9 9) reflection; those on the right column with $\Delta E = 8.5\,\mathrm{meV}$ using the Si (7 7 7) reflection. In the latter column the comparison with a Gaussian lineshape (full line) expected in the free-particle limit is also reported. The vertical dashed line indicates the zero of the energy scale.

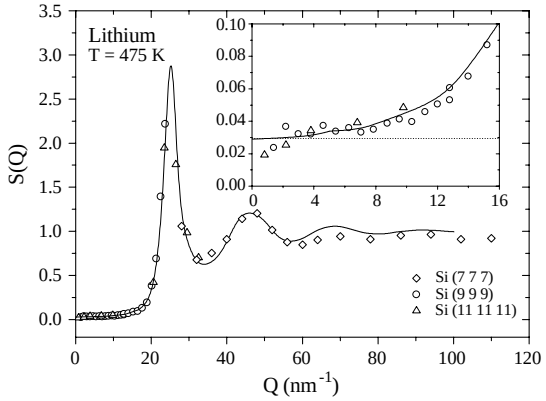

Fig. 2 – Test of normalization accuracy: the $S(Q)$ values as extracted from IXS normalization (open symbols) are reported toghether with computer simulation data (full line) [16]. The inset shows an enlargement of the small-Q region and the dotted line is the $Q \to 0$ limit expected from the isothermal sound velocity.

tering angle, is selected either between 1.4 and 25 nm^{-1} by rotating a 7 m long analyzer arm in the horizontal scattering plane (data taken at $h = 9$ and 11), or between 24 and 110 nm^{-1} by rotating a 3 m long analyzer arm in the vertical scattering plane ($h = 7$). The total Q resolution has been set to 0.4 nm^{-1} at $h = 9$ and 11, and 1 nm^{-1} at $h = 7$. On the horizontal arm, five independent analyzers were used to collect simultaneously five different Q values, determined by the constant angular offset of 1.5° between neighbour analyzers. The vertical arm houses only one analyzer. Energy scans are done by varying the temperature of the monochromator with respect to that of the analyzer crystals. The absolute energy calibration between succesive scans is better than 1 meV. Each scan took about 180 min, and each Q-point spectrum has been obtained from the average of 2 to 8 scans depending on h and the Q-transfer. The data have been normalized to the intensity of the incident beam. The liquid lithium uncapped container is made out of austenitic stainless steel with a resistance heater, used to keep the liquid at $T = 475$ K. The 20 mm long sample, kept together by surface tension, was maintained in a 10^{-6} bar vacuum. The lithium has been loaded in an argon glove box. In the Q-E region of interest, empty vacuum chamber measurements gave either the flat electronic detector background of 0.6 counts/min or, at $9 < Q < 13$ nm^{-1}, a small elastic line due to scattering from the chamber kapton windows (each 50 mm thick) which was subtracted from the data.

The IXS spectra of liquid lithium are reported in fig. 1 at the indicated Q transfer values. The ratio of the intensities of the energy loss (Stokes) and energy gain (anti-Stokes) sides of each spectrum satisfies the detail balance. The low-Q data show the Brillouin triplet structure with the energy of the inelastic peaks increasing with Q up to a Q value of 12 nm^{-1}. This value corresponds to $Q_{\mathrm{M}}/2$, as deduced from the $S(Q)$ reported in fig. 2. One can interpret, therefore, the dispersion up to $Q_{\mathrm{M}}/2$ as that of the longitudinal acoustic branch in the pseudo-first BZ, in agreement with previous findings [12]. The present data, however, allow to establish also that, similarly to what is found in the second BZ of a crystal, in liquid lithium the energy of the acoustic modes decreases with increasing Q from $Q_{\mathrm{M}}/2$ to Q_{M}. Moreover, increasing Q above Q_{M}, *i.e.* in the "third" or higher BZs, one finds that the spectrum gets increasingly broader and distinct peaks are no longer observable. At the highest Q values one finds that the $S(Q, E)$ becomes a symmetric peak centered at energies larger than $E = 0$, as emphasized by the dashed line in fig. 1. Beside the observation of dispersion in a first and second pseudo-

BZs, one also notes that the broadening of the excitations monotonically increases with Q, and towards the end of the second pseudo-BZ, the inelastic features are no longer showing a well-defined peak.

The previous qualitative description can be made substantially more quantitative considering that the dynamic structure factor $S(Q,E)$ can be derived from the measured intensity, $I(Q,E)$, using the zeroth and first moment sum rules for $S(Q,E)$:

$$m^S_{(0)} = \int S(Q,E)\mathrm{d}E = S(Q), \tag{1}$$

$$m^S_{(1)} = \int ES(Q,E)\mathrm{d}E = \hbar^2Q^2/2M\,. \tag{2}$$

We consider that $I(Q,E) = \alpha(Q)\int \mathrm{d}E' S(Q,E')R(E-E')$, where $R(E)$ is the experimental resolution function and $\alpha(Q)$ is a factor taking into account the scattering geometries/efficiencies and the lithium atomic form factor. Consequently, the first moments of the experimental data, $m^I_{(0)}$ and $m^I_{(1)}$, and those of the resolution function, $m^R_{(0)}$ and $m^R_{(1)}$, are related to $m^S_{(0)}$ and $m^S_{(1)}$ by

$$m^I_{(0)} = \alpha(Q)m^S_{(0)}m^R_{(0)}, \tag{3}$$

$$m^I_{(1)} = \alpha(Q)(m^S_{(0)}m^R_{(1)} + m^S_{(1)}m^R_{(0)})\,. \tag{4}$$

From the previous equation one derives that

$$S(Q) = \frac{\hbar^2Q^2}{2M}(m^I_{(1)}/m^I_{(0)} - m^R_{(1)}/m^R_{(0)})^{-1}\,. \tag{5}$$

This procedure has been utilized to put the $S(Q,E)$ on an absolute scale using the experimentally determined $I(Q,E)$ and $R(E)$. The reliability of this procedure is shown in fig. 2, where we obtain an excellent agreement between the $S(Q)$ values obtained by eq. (4) and those derived by Molecular Dynamics (MD) simulation [16].

The possibility to express $S(Q,E)$ in absolute units allows to compare the IXS data with the Gaussian lineshape expected for the $S(Q,E)$ when the single-particle limit is reached. This comparison is reported on the right-hand side of fig. 1, where each solid line represents the sum of two Gaussians:

$$G(Q,E) = \frac{1}{\sqrt{2\pi}}\sum_{i=6,7}\frac{C_i}{\sigma_i}\exp[-(E-E_i)^2/2\sigma_i^2]\,, \tag{6}$$

where $C_6 = 0.08$ and $C_7 = 0.92$ are the natural abundances of the ^{6}Li and ^{7}Li isotopes, $E_i = \hbar^2Q^2/2M_i$ their recoil energies and $\sigma_i^2 = \hbar^2K_\mathrm{B}TQ^2/M_i$. The progressively better agreement between the data and $G(Q,E)$ with increasing Q testifies the evolution towards the single-particle behaviour, which seems to be reasonably well reached at the highest investigated Q values and at the considered temperature.

The dispersion relation of the energy $\Omega(Q)$ of the inelastic signal observed in fig. 1 is obtained by determining the maximum of the current spectra. This allows us to accurately estimate $\Omega(Q)$ independently of any specific model for the $S(Q,E)$. The values of $\Omega(Q)$ have been determined by a parabolic fit of the maximum region in the Stokes side. The values of $\Omega(Q)$ are reported in fig. 3, and their statistic uncertainties are systematically smaller than the utilized symbols. In fig. 3a are also reported the linear dispersion of the adiabatic sound velocity (dotted line) and the dispersion expected for the single-particle dynamics [17]. We observe that $\Omega(Q)$ is close to the adiabatic sound mode at the lowest Q values, and it

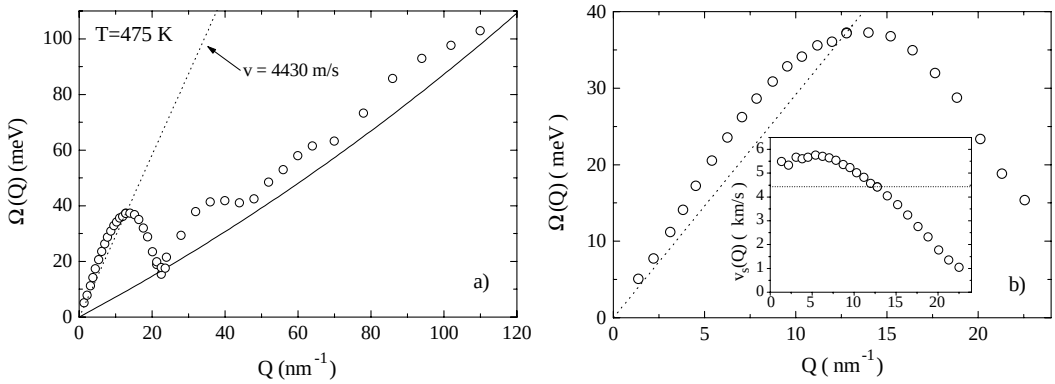

Fig. 3 – Sound dispersion of lithium. a) The energy position of the Stokes Peak of the Current Correlation Function (open circles) are reported toghether with the dispersion expected in two limiting cases: low-Q linear dispersion with hidrodynamic velocity (dotted line) and high-Q dispersion (full line) of the impulse approximation. These two dispersion curves have been computed assuming the presence of both ^{6}Li and ^{7}Li in their natural abundances (see text and eq. (6)). b) Detail of the "small Q" (below the First Sharp Diffraction Peak) region. The deviation of the acoustic sound velocity from the adiabatic value (dotted line) at increasing wave vectors is observed (positive dispersion).

always shows a positive dispersion before reaching the maximum of the first pseudo-BZ. This is emphasized in fig. 3b, where the low-Q region is expanded, and the inset reports directly the sound velocity $v(Q) = \Omega(Q)/Q$. The observation of a positive dispersion confirms previous MD [18–21] and experimental [12] data in a similar Q region on lithium and other alkali liquid metals. However, contrary to the findings reported in ref. [12], where the transition between the two regimes takes place above $3.6\,\mathrm{nm}^{-1}$, the increased energy resolution of the present work allows to firmly establish that the hydrodynamic regime is not yet reached at the lowest investigated Q value, $1.4\,\mathrm{nm}^{-1}$. This discrepancy cannot be explained even considering that in ref. [12] the considered dispersion was erroneously obtained from the maxima of $S(Q, E)$ rather than from those of the current spectra, as done here, and is probably due to the substantial less accuracy of the old data.

Considering higher Q values, the points in fig. 3a show not only a second pseudo-BZ, as already pointed out in fig. 1, but also a series of oscillations that damp out with increasing Q —here, $\Omega(Q)$ approaches the single-particle line. These oscillations are in anti-phase with the oscillations found in the $S(Q)$ (see fig. 2) and can, therefore, be associated to the local order in the liquid. A further great interest in these data is to be able to follow all the way, from the sound mode to the free-particle, regime the evolution of $\Omega(Q)$. Beside the importance of a unified picture in such a wide Q region, these data provide, in fact, the workbench for a quantitative theoretical analysis of the shape of the $S(Q, E)$. Moreover, they clearly show the existence of high-order pseudo-BZ in a liquid; such kind of information has only been found so far in liquid helium (^{3}He and ^{4}He) from the combination of various neutron experiments —the current spectra maxima and widths have been found to oscillate with Q with a period dictated by the first-neighbour distance, and these observations were suggested to be a quantum interference effect [22].

In conclusion, using IXS, we report a very accurate measure of the $S(Q, E)$ in liquid lithium, reduced to its absolute scale. The large investigated momentum and energy regions, both spanning over two decades, have allowed to determine the collective dynamics of this simple liquid from the collective modes regime, dominated by sound-like excitations, all the way towards the impulse approximation regime, dominated by single-particle dynamics. Moreover, this textbook result shows the effects of the structural correlations in the dynamics of simple

liquids: it is in fact possible to identify in a liquid features qualitatively similar to those of phonons in the BZs of crystals.

* * *

We acknowledge valuable help of H. Mueller from the Chemistry Laboratory at ESRF for his technical assistance during the sample manipulation.

REFERENCES

[1] Boon J. P. and Yip S., *Molecular Hydrodynamics* (McGraw-Hill, New York) 1980.
[2] Balucani U. and Zoppi M., *Dynamics of the Liquid State* (Clarendon Press, Oxford) 1994.
[3] Lovesey S. W., *Z. Phys. B*, **58** (1985) 79.
[4] Silver R. N. and Sokol P. E., *Momentum Distributions* (Plenum Press, New York) 1989.
[5] De Jong P. H. K., PhD thesis, Technische Universiteit Delft, The Netherlands (1993).
[6] De Jong P. H. K., Verkerk P. and De Graaf L. A., *J. Non Cryst. Solids*, **156-158** (1993) 48.
[7] van Well A. A., Verkerk P., de Graaf L. A., Suck J. B. and Copley J. R. D., *Phys. Rev. A*, **31** (1985) 3391; van Well A. A. and de Graaf L. A., *Phys. Rev. A*, **32** (1985) 2396; Bafile U., Verkerk P., Barocchi F., de Graaf L. A., Suck J. B. and Mutka H., *Phys. Rev. Lett.*, **65** (1994) 2394.
[8] Copley J. R. D. and Rowe M., *Phys. Rev. A*, **9** (1974) 1659; Morkel C. and Glaser W., *Phys. Rev. A*, **33** (1986) 3383; Verkerk P., De Jong P. H. K., Arai M., Bennington S. M., Howells W. S. and Taylor A. D., *Physica B*, **180-181** (1992) 834; Novikov A. G., Savostin V. V., Shimkevich A. L. and Yulmetiev R. M., *Physica B*, **228** (1996) 312; Chieux P., Dupuy-Philon J., Jal J. F. and Suck J. B., *J. Non Cryst. Solids*, **205-207** (1996) 370.
[9] Lovesey S. W., *Theory of Neutron Scattering from Condensed Matter* (Clarendon Press, Oxford) 1994, p. 120.
[10] Burkel E., *Inelastic Scattering of X-rays with Very High Energy Resolution* (Springer Verlag, Berlin) 1991, and references therein.
[11] Sette F., Krisch M., Masciovecchio C., Ruocco G. and Monaco G., *Science*, **280** (1998) 1550; Ruocco G. and Sette F., *J. Phys. Condens. Matter*, **11** (1999) R259.
[12] Sinn H., Sette F., Bergmann U., Halcoussis Ch., Krisch M. and Verbeni R., *Phys. Rev. Lett.*, **78** (1997) 1715.
[13] Oshe R. *et al.* (Editors), *Handbook of Thermodynamic and Transport Properties of Alkali Metals* (Blackwell Scientific Publications) 1985, p. 735.
[14] Verbeni R., Sette F., Krish M., Bergman U., Gorges B., Halcoussis C., Martel K., Masciovecchio C., Ribois J. F., Ruocco G. and Sinn H., *J. Synchr. Radiat.*, **3** (1996) 62.
[15] Masciovecchio C., Bergman U., Krish M., Ruocco G., Sette F. and Verbeni R., *Nucl. Instrum. Methods B*, **111** (1986) 181; **117** (1986) 339.
[16] Scopigno T., private communication.
[17] This function is obtained by solving the equation $\partial[E^2 G(Q,E)]/\partial E = 0$. For a single isotope system, its analytical expression is given by $\Omega(Q) = (E_i(Q) \pm \sqrt{E_i(Q)^2 + 8\sigma_i^2})/2$, with the $\pm$ signs referring to Stokes and anti-Stokes components, respectively. In our two isotopes systems, the equation has been solved numerically.
[18] Rahman A., *Phys. Rev. Lett.*, **32** (1974) 52.
[19] Bodensteiner T., Morkel C., Glaser W. and Dorner B., *Phys. Rev. A*, **45** (1992) 5709.
[20] Canales M., Gonzales L. E. and Padro J. A., *Phys. Rev. E*, **50** (1994) 3656.
[21] Torcini A., Balucani U., de Jong P. H. K. and Verkerk P., *Phys. Rev. E*, **51** (1995) 3126.
[22] Glyde H. R., *Excitations in Liquid and Solid Helium* (Clarendon Press, Oxford) 1990, p. 356.